



Liquid-phase catalytic hydroxylation of phenol using metal crosslinked alginate catalysts with hydrogen peroxide as an oxidant



Fengwei Shi^a, Li Mu^b, Peng Yu^c, Jianglei Hu^a, Long Zhang^{a,*}

^a School of Chemical Engineering, Changchun University of Technology, Changchun 130012, PR China

^b School of Bioscience and Technology, Changchun University, Changchun 130023, PR China

^c Petrochina Jilin Petrochemical Company Acrylonitrile Factory, Jilin 132021, PR China

ARTICLE INFO

Article history:

Received 12 October 2013

Received in revised form 5 April 2014

Accepted 5 April 2014

Available online 15 April 2014

Keywords:

Metal crosslinked alginate

Dry bead

Phenol hydroxylation

Heterogeneous catalysts

ABSTRACT

A series of divalent metal (Cu, Co, Ni, Fe, Mn, Zn and Pd) crosslinked alginate dry beads catalysts were prepared using metal chloride and sodium alginate. The resulting catalysts were characterized by Fourier transform infrared spectroscopy, X-ray photoelectron spectroscopy, inductively coupled plasma atomic emission spectroscopy, scanning electron microscopy, energy-dispersive X-ray analyses and nitrogen physisorption measurements. The characterization results showed that a series of ion-crosslinked metal-alginate dry beads were synthesized through ion exchange, followed by the coordination of alginate and metal ions. These materials have been assessed as catalysts for liquid-phase hydroxylation of phenol to dihydroxybenzenes using H₂O₂ as an oxidant. The results showed that Cu-based catalyst exhibited higher activity than other metal-based catalysts for phenol hydroxylation. The influence of key reaction parameters, including the reaction temperature, solvent, reaction time, initial pH, molar ratio of phenol/H₂O₂ and the amount of catalyst on the reactivity and selectivity were also investigated. Finally, the reusability of Cu-based catalyst illustrated that it could be recovered and reused without notable loss of activity.

© 2014 Published by Elsevier B.V.

1. Introduction

The products of phenol hydroxylation are hydroquinone (HQ) and catechol (CAT), of which the scientific importance and commercial value is demonstrated by their applications in pharmaceuticals, drugs, polymerization inhibitors, photography and so on [1–4]. The most desirable method for producing dihydroxybenzenes is direct hydroxylation of phenol with hydrogen peroxide. Hydrogen peroxide which has high active oxygen content has been widely explored as a green oxidant in oxidation reactions, because it is readily available and the resulting products are water and oxygen, which are environment-friendly [5]. For the hydroxylation reaction, many homogeneous and heterogeneous catalysts have been studied. While homogeneous catalysts such as mineral acids, metal ions and metal complexes are difficult to be separated and recovered from the reaction mixture, which prevent their applications in practical utilization. Compared with homogeneous catalysts, heterogeneous catalysts such as zeolites [6,7], heteropolyacids [8], metal oxides [9], hydrotalcite-like compounds [10–12],

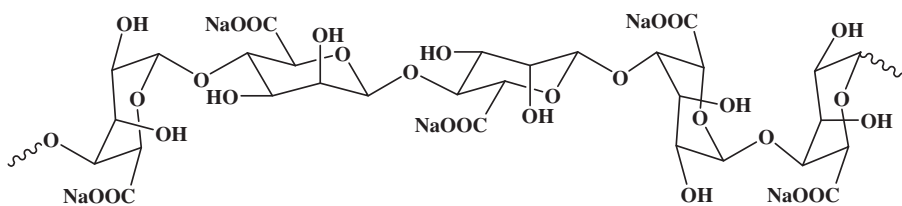
nanoparticles [13] and mesoporous materials [14,15] have been widely utilized in phenol hydroxylation reaction because of their favorable activities, selectivities and easy separation [16–19]. Therefore, the design of suitable heterogeneous catalysts for hydroxylation reaction has been an important area of research. However, there are also some problems with the preparation and utilization of these catalysts, such as complexity, high cost and toxicity involved in the process. Consequently, the present research focuses on exploring new catalysts which are cheap, widely abundant and environment-friendly.

Alginate is both a biopolymer and a polyelectrolyte that is considered to be biocompatible, non-toxic, non-immunogenic and biodegradable [20]. It can be characterized as an anionic copolymer comprised of (1 → 4)-linked β-D-mannuronic (M) and α-L-guluronic (G) residues [21–23]. In Scheme 1, the M and G blocks of the alginate with their representative sequence are reported. Because alginate has a number of free hydroxyl and carboxyl groups distributed along the backbone, it is an ideal candidate for chemical functionalization, and has good adsorption capacity for metals cations (e.g. Ca²⁺, Ba²⁺, Co²⁺, Cu²⁺, Ni²⁺ and Fe²⁺, except Mg²⁺) [24–26]. As well, alginate can be shaped as self-standing beads, films or monoliths with good mechanical stability [21]. Thus, the alginate became a desirable metal catalyst carrier and had been utilized in some catalytic reactions [27–29]. However, few reports

* Corresponding author at: Yan'an Street No. 2055, Changchun, China.

Tel.: +86 431 85716785; fax: +86 431 85716785.

E-mail addresses: hujl863@163.com (J. Hu), zhanglongzh@163.com (L. Zhang).

**Scheme 1.** Molecular structure of sodium alginate.

focused on the synthesis and utilization of metal alginates as catalysts for the hydroxylation of phenol.

In the current study, a process was designed to prepare a series of metals crosslinked alginate (M-ALG) dry beads catalysts (**Scheme 2**). These coordination polymers were well-characterized by inductively coupled plasma atomic emission spectroscopy (ICP-AES), Fourier transform infrared spectroscopy (FT-IR), UV-vis diffuse reflectance spectroscopy (UV-vis/DRS), scanning electron microscopy (SEM), energy-dispersive X-ray (EDX), X-ray photoelectron spectroscopy (XPS) and nitrogen sorption analysis, to prove the formation of the coordination binding between metal ion and alginate, and to explore the morphology and surface textural property of the prepared catalysts. The catalysts were subsequently applied in phenol hydroxylation with H_2O_2 as an oxidant under mild reaction conditions. The influence of key reaction parameters for this reaction was investigated, and the reusability of the catalysts was evaluated.

2. Experimental

2.1. Materials

All chemicals used were of analytical grade, sodium alginate, copper chloride dehydrate ($CuCl_2$), cobalt chloride tetrahydrate, manganese chloride tetrahydrate, ferrous chloride dehydrate, nickel chloride hexahydrate, zinc chloride, palladium chloride, hydrogen peroxide (wt. 30%) were obtained from Tianjin Guangfu Fine Chemical Research Institute, Tianjin China. Phenol, catechol, hydroquinone and benzoquinone were obtained from Aldrich. All chemicals were used without further purification.

2.2. Catalyst preparation

2.2.1. Synthesis of M-ALG, M=Co, Ni, Fe, Mn, Zn or Pd

The divalent metal (Co, Ni, Fe, Mn, Zn and Pd) chloride solutions with molar concentration of 0.3 mol/L were prepared in 100 mL distilled water. Sodium alginate was dissolved in distilled water at a concentration of 4% (w/v) and then dropped into the former metal chloride solutions through a syringe with a 2 mm-diameter needle. The reaction proceeded at 50 °C for 6 h with a gentle stirring (200 rpm) to form gel beads, and then these gel beads were separated from the solution and washed with distilled water. After dried

at 40 °C for 3 days, the dry beads were obtained. The above catalysts were denoted as M-ALG-3.

2.2.2. Synthesis of Cu-ALG

Four $CuCl_2$ solutions with different concentrations (0.1, 0.2, 0.3 and 0.4 mol/L) were used to prepare the Cu-ALG by following the above way. The prepared catalysts were denoted as Cu-ALG-x, where $x = 1, 2, 3$ and 4 represent the molar concentration of $CuCl_2$ being 0.1, 0.2, 0.3 and 0.4 mol/L, respectively.

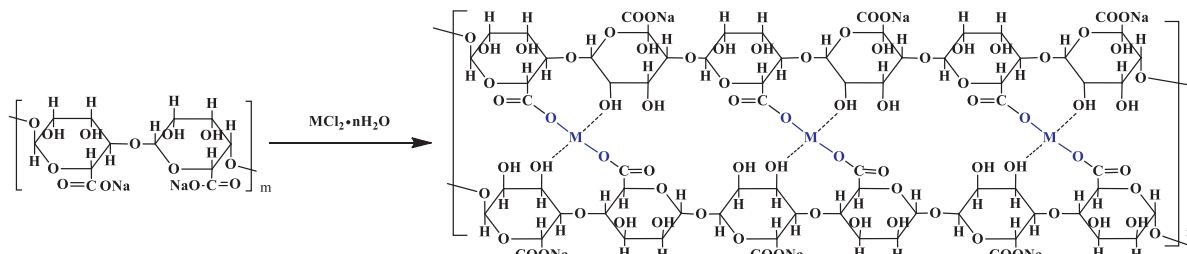
2.3. Characterization of the sample

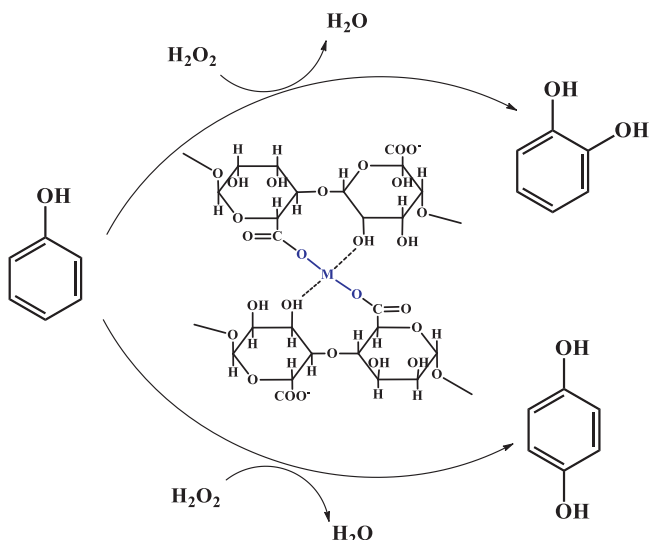
FT-IR spectra were recorded on a Nicolet IS10 IR spectrophotometer with n of scans to be 32, and the spectra were collected within the range of 400–4000 cm^{-1} . UV-vis/DRS were recorded at ambient atmosphere in the wavelength range of 200–800 nm using a Hitachi U-4100 spectrometer. The contents of metal elements in the alginates were determined by a Leeman Prodigy Spec ICP-AES. All determinations were conducted at least in triplicate. The external morphology of the dry beads was examined using a JEOL JSM-5600LV SEM with an EDX system (EDAX-Falcon). The nitrogen adsorption/desorption measurement was performed on a Micromeritics ASAP 2020 M surface area and porosity analyzer. XPS was performed in Thermo ESCALAB 250 spectrometer.

2.4. Activity test of the catalyst

Phenol hydroxylation with H_2O_2 was carried out in a three-necked round bottom flask equipped with mechanical stirrer and reflux condenser (**Scheme 3**). First, 1.0 g (10 mmol) of phenol was dissolved in 30 mL of distilled water, and set amount of catalyst was added. Then, H_2O_2 (30%) was added within 30 min. The amount of H_2O_2 introduced was varied to obtain a desired phenol/ H_2O_2 ratio. After a given reaction time, initial pH and temperature, the resulting mixture was sampled. The products were analyzed by gas chromatography (Agilent GC6890) through a HP-5 column (film thickness, 0.25 μ m; i.d., 0.25 mm; length, 30 m) using a flame ionization detector (FID) and the concentration of residual H_2O_2 was determined by the iodometric titration.

The performance of the catalysts is evaluated quantitatively by the conversions of phenol and H_2O_2 , the selectivities to catechol (CAT), hydroquinone (HQ) and para-benzoquinone (BQ), and turnover frequency (TOF: moles of reacted substrate over moles

**Scheme 2.** Pathway of the synthesis of M-ALG dry beads catalysts.



Scheme 3. Hydroxylation of phenol to produce CAT and HQ with H₂O₂ catalyzed by M-ALG.

of metal per hour) obtained at the selected conditions. Herein, the conversion of phenol is expressed by X_{phenol} :

$$X_{\text{phenol}}(\%) = 100 \times (C_{\text{b,phenol}} - C_{\text{a,phenol}})/C_{\text{b,phenol}}$$

where $C_{\text{b,phenol}}$ and $C_{\text{a,phenol}}$ are the molar concentrations of phenol before and after the reaction, respectively. The selectivity of the product is shown by S_p :

$$S_p(\%) = 100 \times C_p/(C_{\text{b,phenol}} - C_{\text{a,phenol}})$$

where C_p is the molar concentration of the product and $p = \text{CAT, HQ or BQ}$. The conversion of H₂O₂ is shown by $X_{\text{H}_2\text{O}_2}$:

$$X_{\text{H}_2\text{O}_2}(\%) = 100 \times (C_{\text{b,H}_2\text{O}_2} - C_{\text{a,H}_2\text{O}_2})/C_{\text{b,H}_2\text{O}_2}$$

where $C_{\text{b,H}_2\text{O}_2}$ and $C_{\text{a,H}_2\text{O}_2}$ are the molar concentrations of H₂O₂ before and after the reaction, respectively.

3. Results and discussion

3.1. Catalyst characterization

3.1.1. FT-IR spectral studies

The FT-IR spectra revealed the changes in the absorption bands for the surface functional group of the sodium alginate before and after reacting with the cationic solution (Fig. 1). The broad absorption band around 3400 cm⁻¹ was due to the stretching vibrations of the hydroxyl groups. In this study, the peak shifted from 3400 cm⁻¹ to higher wavenumber after sodium alginate reacted with cations to form the metal crosslinked alginates dry beads. The increase in the adsorption peak should be attributed to the attachment of the metal cations to the -OH group. The spectrum of Na-ALG showed the absorption bands at 1639 and 1386 cm⁻¹, which were assigned to asymmetric and symmetric stretching peaks of the carboxylate salt groups. While after crosslinking, both the C=O and C—O in the carboxyl group (-COO⁻) shifted slightly in frequency. The red-shifting of the C=O bond could be attributed to the C—O coordination with the metal cations, which led to the decrease in the stretching force constant of the carboxyl group [30]. In addition, the C—O in the carboxyl group bond shifted to a higher frequency, which was attributed to the coordination of metal cations to the carboxylate ion (-COO⁻), as well the high electron density induced by the cations sorption onto the adjacent hydroxyl group.

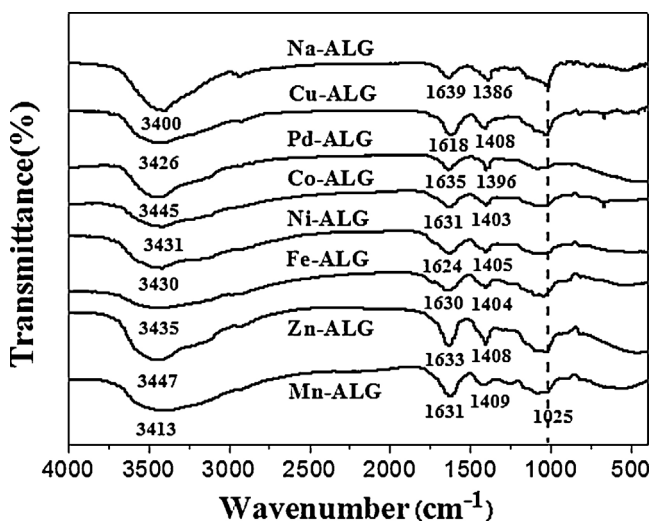


Fig. 1. FT-IR spectra of M-ALG dry beads.

Usually, the identification of the different oxidation states of the transition metals in compounds can be easily carried out by XPS because the different shapes or energy position of the photoelectrons. The XPS spectra of the M-ALG were shown in Fig. 2a–g. It is known that the appearance of spin-orbit split of Cu ($2p_{3/2}$ and $2p_{1/2}$) along with their shake up satellites is mainly a characteristic of bivalent copper (Fig. 2a) [31]. The Cu ($2p_{3/2}$ and $2p_{1/2}$) peaks were at 935.2 and 955.2 eV, separated by 20.0 eV, indicating the Cu in the catalyst was mainly Cu²⁺. Regarding Mn, Co, Ni, Zn and Fe-ALG, the separated binding energy of their $2p_{3/2}$ and $2p_{1/2}$ peaks were 11.7, 15.5, 18.4, 23.1 and 13.6 eV, respectively (Fig. 2b–f) [32–34], indicating the chemical valence of these metals were all bivalent. The XPS analysis results of the Pd 3d were shown in Fig. 2g. It was characterized by the two spin-orbit split of Pd $3d_{5/2}$ (343.3 eV) and Pd $3d_{3/2}$ (339.0 eV), separated by 5.3 eV, indicating that the Pd ions in the catalyst were bivalent [35].

SEM image in Fig. 3 were taken at 50× and 1000× magnifications to observe the external and internal morphology of the dry beads, respectively. As shown in Fig. 3A, the Cu-ALG dry bead was in spherical form and had a very rough surface, on which some macropores or roughness could be found. Compared with the gel beads, the dry beads were more compact, which enhanced the mechanical stability. The stratified structures were found on the surface of the blocks (Fig. 3B). As the gel beads dried, the interior shrank to a greater extent than the exterior regions, giving this kind of "crumpled" structure with decreased size without affecting surface area significantly [36]. If the dry bead was cut (Fig. 3C), it could be found that the centre of the bead was solid, which was consistent with Fernandez's report [37].

Table 1
The content of metal in alginate catalysts before and after reaction.

Entry	Catalysts	Metal content (before reaction)/%	Metal content (after reaction)/%
1	Mn-ALG-3	13.1	12.9
2	Co-ALG-3	12.5	12.4
3	Fe-ALG-3	11.6	11.4
4	Ni-ALG-3	11.7	11.5
5	Zn-ALG-3	13.5	13.4
6	Pd-ALG-3	12.7	12.6
7	Cu-ALG-1	9.7	9.4
8	Cu-ALG-2	14.1	13.7
9	Cu-ALG-3	15.3	15.2
10	Cu-ALG-4	15.5	15.2

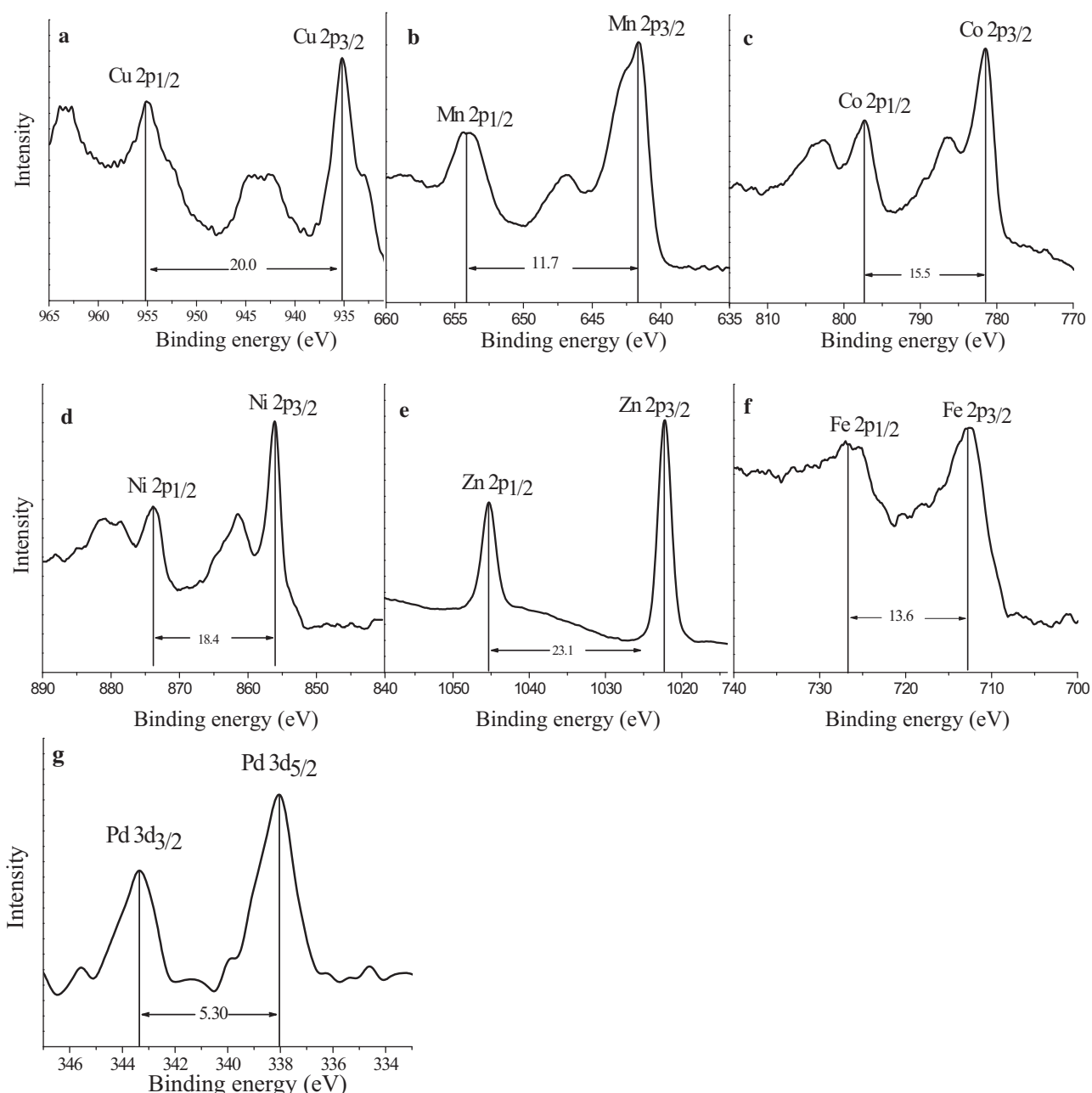


Fig. 2. XPS spectra of (a) Cu-ALG, (b) Mn-ALG, (c) Co-ALG, (d) Ni-ALG, (e) Zn-ALG, (f) Fe-ALG and (g) Pd-ALG.

The EDX spectrum of Cu-ALG dry beads analyzed by using elemental microprobe method of SEM/EDX was illustrated in Fig. 4. From Fig. 4a, it could be found that only O, C, Cu and Cl signals were observed on the surface of catalyst, while Na signals could be found only in the centre of the catalyst (Fig. 4b), which demonstrated that Na ions on the surface of the catalyst had been exchanged completely. EDX analysis therefore provided the direct evidence for crosslinking of the Cu on the surface of alginates.

As SEM coupled EDX microprobe analysis is semi-quantitative analysis, to precisely investigate the metals contents of the catalysts, ICP-AES was applied (Table 1). Table 1 showed that different metal elements had different crosslinked content with alginate, among which the Cu content was the highest (reached to 15.3%), and for the other dry beads, the crosslinked contents of metals were between 11.6% and 13.5%. The results illustrated that the ability of alginate crosslinking with metal was different.

In order to detect the relation of metal in catalyst and raw material, a series of Cu-ALG dry beads were prepared using different concentration of CuCl₂ (0.1–0.4 mol/L), the results (Table 1, entries 7–10) showed that the Cu content of the Cu-ALG dry beads increased with the increase of the CuCl₂ concentration. When the CuCl₂ concentration increased from 0.1 to 0.3 mol/L (Table 1, entries 7–9), the Cu content of the dry beads increased significantly (from 9.7% to 15.3%). However, when the CuCl₂ concentration exceeded 0.3 mol/L, the change of the Cu content in dry beads was unapparent. This result should be attributed to the saturation of the crosslinked products [29]. To test whether metal ions were leaching out from the catalysts, ICP-AES was used to detect the metals contents after once hydroxylation reaction. The results showed that a trace amount of metals was lost (lower than 3 wt.%) during the phenol hydroxylation reaction.

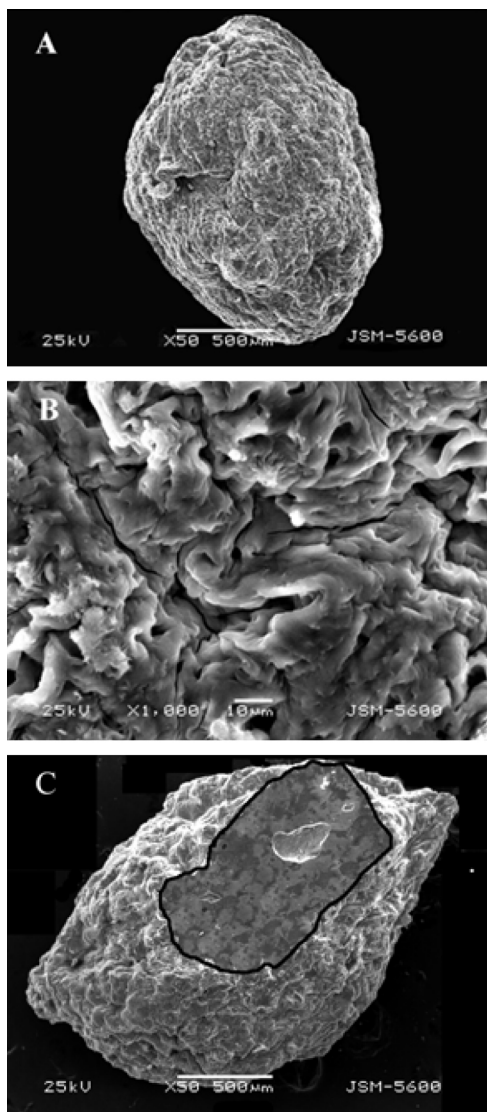


Fig. 3. SEM images of Cu-ALG.

Besides, the elemental concentration distribution of the Cu-ALG dry beads can be analyzed using the mapping analysis of SEM/EDX. The Cu ions distribution mapping by EDX analysis of the catalyst before and after regeneration (The spent catalyst was recovered by filtration, washed thoroughly with ethanol and dried.) of hydroxylation was illustrated in Fig. 4c and d. The bright white points represented the signal of Cu element on the surface of the dry beads. The result showed that after hydroxylation and regeneration, the amount of Cu ions on the surface of the catalyst reduced insignificantly, which was consistent with the ICP-AES.

To investigate the specific surface area and porosity of the prepared alginate dry beads, a BET test was performed. The results of nitrogen sorption ($<1 \text{ cm}^3/\text{g}$) and surface area ($<1 \text{ m}^2/\text{g}$), calculated by the BET method, indicated that the dry beads have no small dimensions pores [38], which was consistent with the SEM result. Thus, the sags on the surface were likely caused by the depressions of the surface, which occurred during the drying phase.

3.2. Catalytic phenol hydroxylation

3.2.1. Catalytic behaviors of various catalysts

Liquid-phase hydroxylation of phenol catalyzed by the metal crosslinked alginate using H_2O_2 as an oxidant has been studied.

Two major products (CAT and HQ) and a small amount of byproduct (BQ) were identified by GC. The catalytic performance of various transition metals (Cu, Co, Ni, Fe, Mn, Zn and Pd) alginates catalysts in phenol hydroxylation was listed in Table 2. The conversion of phenol, conversion of H_2O_2 and turnover frequency (TOF: moles of reacted substrate over moles of metal per hour) were used to evaluate the catalytic activities of prepared catalysts. The result of a blank experiment under the same reaction conditions showed that in the absence of the catalyst, H_2O_2 alone was unable to oxidize phenol to a significant extent (only 5.3%, entry 1) [39]. After the prepared catalysts were added, the conversions of phenol were increased in all experiments (entries 2–11). While concerning with Mn-ALG, Zn-ALG and Pd-ALG (entries 2–4), the conversion of phenol increased little, which indicated the low activities of them in the hydroxylation reaction. For the Co, Fe, Ni and Cu alginates (entries 5–7 and entry 10), obvious increases in conversions were observed. Prepared with the same concentration of chloride (0.3 mol/L), their reactivities (conversion of phenol, conversion of H_2O_2 , and TOF) followed the order: Cu-ALG-3 > Fe-ALG-3 > Ni-ALG-3 > Co-ALG-3, and the selectivities to dihydroxybenzenes were nearly the same (above 97%). Transition metal complexes are known to have effect on the decomposition of H_2O_2 either by a free radical mechanism or through the formation of active peroxy species in the coordination sphere [40]. Because the decomposition behavior of H_2O_2 in oxidation is resulted by the electronic and steric factors of the transition metal, the difference of the activities of these catalysts could be due to the different transition metals chosen.

With regard to the Cu-ALG-x catalysts (entries 8–11) [39], the conversion was increased as the Cu content increased. When the concentration of CuCl_2 increased from 0.1 to 0.3 mol/L (entries 8–10, the loaded Cu content increased from 9.7% to 15.3%, entries 7–11 in Table 1), the TOF value changed little, while the conversions of phenol and H_2O_2 increased from 33.1% to 52.7% and 88.2% to 96.7%, respectively, with a catechol-to-hydroquinone ratio of 3:2, which is higher than the value reported in the literature [18,41]. It is believed that a large number of Cu active sites increased the decomposition rate of H_2O_2 [29]. The conversion changed little when the concentration of CuCl_2 reached to 0.4 mol/L (entry 11, the loaded Cu content reached 15.5%), which was likely to be attributed to the saturation of Cu-ALG. This result was consistent with the results of ICP-AES.

3.2.2. Catalytic behaviors under different reaction conditions

To investigate the influence of the reaction conditions of the catalyst on the catalytic activity of phenol hydroxylation, the Cu-ALG-3 catalyst was used to conduct the experiment. The effects of solvent, temperature, reaction time, molar ratio of phenol/ H_2O_2 , the amount of catalyst, initial pH, catalyst stability and reusability on conversion profiles were examined in detail.

3.2.2.1. The influence of solvents. It is well-known that the solvent plays an important and sometimes decisive role in the catalytic behavior of a catalyst [42,43]. The effect of solvents (ethanol, acetonitrile, ethyl acetate and water) has been investigated in the reaction. As listed in Table 3, the catalytic activities were strongly dependent on the solvents. The conversion of phenol was 52.7% with a catechol-to-hydroquinone ratio of 3:2 in water, which was better than in other organic solvents. In ethanol, acetonitrile and ethyl acetate, the conversion of phenol was very low that the catalytic activities could be almost ignored. The polarity order of the solvents is water > acetonitrile > ethanol > ethyl acetate, and the hydroxyl radicals is more stable in polar solvents. Considering the above results, it was found that polar solvent could promote the oxidation of phenol, which suggested that the radical reaction

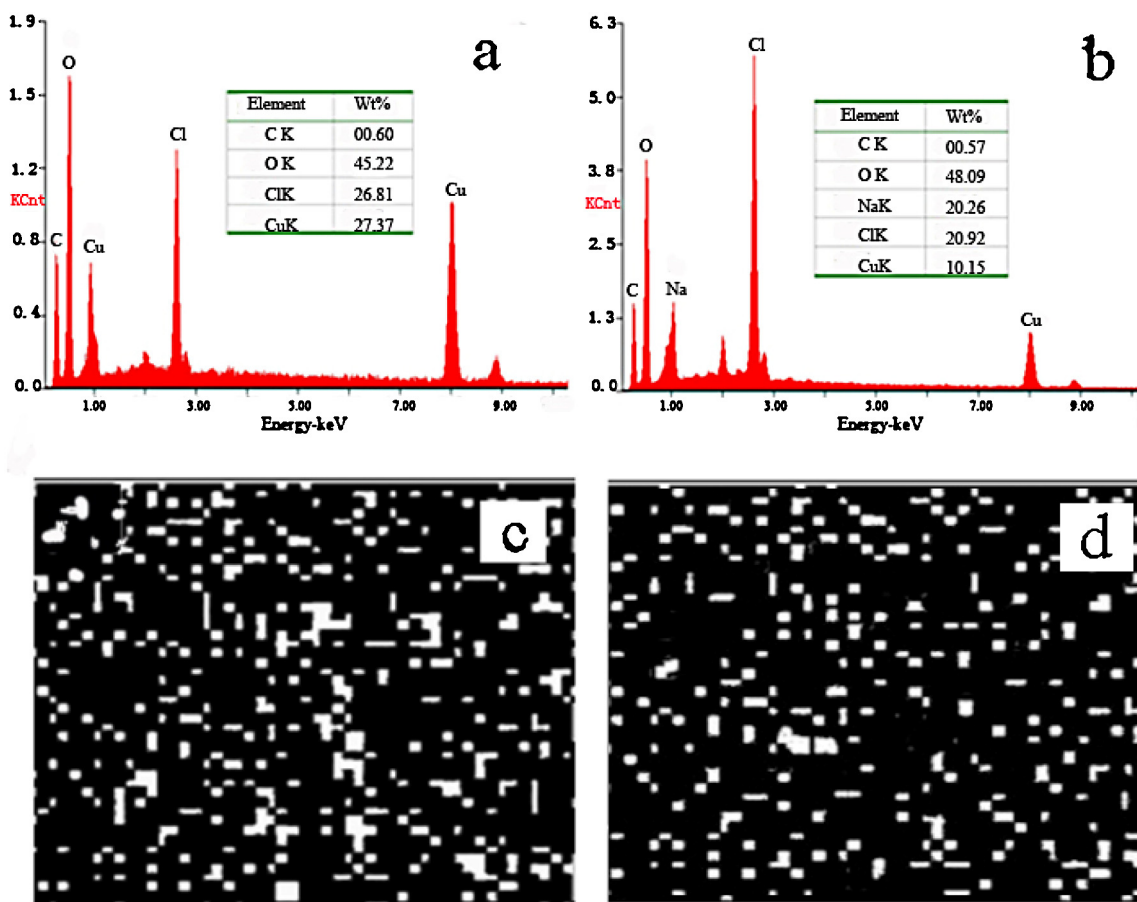


Fig. 4. EDX analysis of (a) surface of the Cu-ALG; (b) centre of the Cu-ALG; mapping of Cu element in Cu-ALG catalyst before (c) and after regeneration of (d) hydroxylation reaction.

mechanism was in operation on phenol hydroxylation over these catalysts.

3.2.2.2. The influence of temperature. The effect of the reaction temperature on the conversion of phenol, the selectivity of dihydroxybenzene in the range from 20 to 80 °C was showed in Fig. 5. It could be found that the reaction temperature was an important parameter. When the temperature increased from 20 to 80 °C, the conversion of phenol increased from 22.1% to 55.2%. In addition, the selectivity of dihydroxybenzenes increased with the temperature increasing from 20 to 60 °C. While going on increasing the temperature to 80 °C, the selectivity of dihydroxybenzenes dropped,

because the byproduct of BQ increased. Therefore, the suitable temperature for this catalytic reaction was 60 °C.

3.2.2.3. The influence of reaction time. In the catalytic system, the duration of the hydroxylation reaction was studied within 5 h keeping other parameters constant to optimize reaction time. Generally, the conversion of phenol increased with increasing of reaction time. From the result displayed in Fig. 5, the conversion of phenol increased rapidly within the first 2 h, while when the reaction time increased beyond 2 h, the conversion of phenol increased in a small range. (The conversions of phenol were 52.7%, 53.9% and 54.9%, at 3, 4 and 5 h, respectively.)

Table 2
Catalytic activities and selectivity in phenol hydroxylation.

Entry	Catalyst	$X_{\text{phenol}} (\%)^{\text{a}}$	$X_{\text{H}_2\text{O}_2} (\%)$	Selectivity (%) ^b			TOF (h ⁻¹)
				CAT	HQ	BQ	
1	Blank	5.3	61.4	59.1	38.8	2.1	–
2	Mn-ALG-3	7.2	70.3	52.4	46.7	0.9	0.29
3	Zn-ALG-3	7.8	64.0	55.0	43.8	1.2	0.37
4	Pd-ALG-3	6.3	62.7	57.2	42.4	0.4	0.52
5	Co-ALG-3	39.5	84.4	60.9	36.8	2.3	1.82
6	Ni-ALG-3	41.3	91.2	53.5	44.1	2.4	2.02
7	Fe-ALG-3	44.2	93.9	50.1	47.9	2.0	2.09
8	Cu-ALG-1	33.1	88.2	58.9	38.2	2.9	2.10
9	Cu-ALG-2	48.6	94.0	57.1	40.0	2.9	2.13
10	Cu-ALG-3	52.7	96.7	59.5	38.4	2.1	2.14
11	Cu-ALG-4	52.9	96.8	57.4	40.6	2.0	2.13

^a Phenol, 1.0 g; catalyst, 50 mg; phenol/H₂O₂ molar ratio, 1:2; water, 30 mL; 60 °C; 2 h.

^b Product distribution given on a tar-free basis.

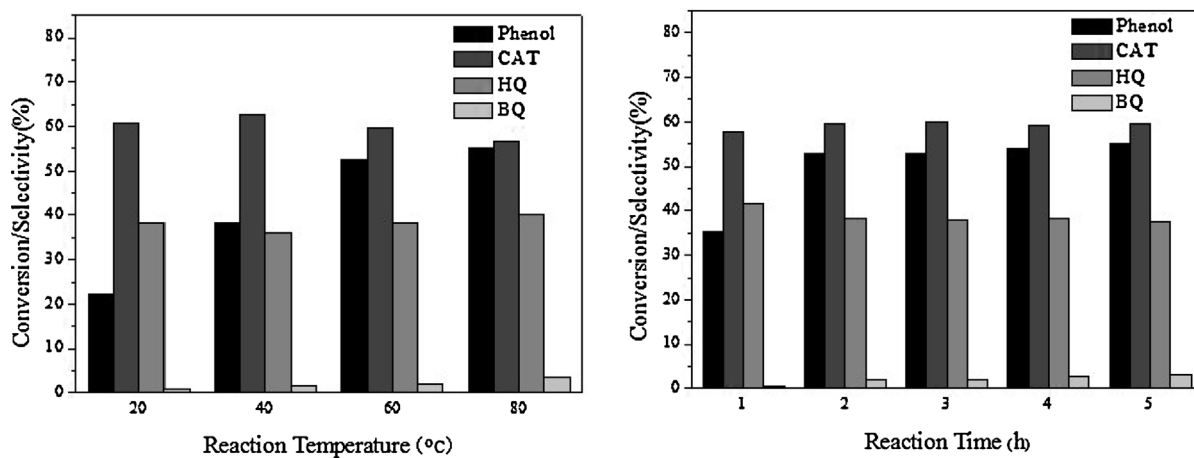


Fig. 5. Temperature and time studied over Cu-ALG-3.

Table 3
Effect of solvents in the phenol hydroxylation catalyzed by Cu-ALG-3.

Solvent	$X_{\text{phenol}} (\%)^{\text{a}}$	Selectivity (%) ^b		
		CAT	HQ	BQ
Water	52.7	59.5	38.4	2.1
Acetonitrile	11.5	27.1	72.7	0.2
Ethanol	7.2	62.3	37.5	0.2
Ethyl acetate	–	–	–	–

^a Phenol, 1.0 g; catalyst, 50 mg; phenol/H₂O₂ molar ratio, 1:2; solvent, 30 mL; 60 °C; 2 h.

^b Product distribution given on a tar-free basis.

The selectivity to hydroquinone decreased with prolonging the reaction time. It is proposed that at the later reaction stage, an oxidation of hydroquinone in the reaction medium with H₂O₂ might cause the formation of *p*-benzoquinone in relatively large amount.

3.2.2.4. The influence of molar ratio of phenol/H₂O₂. The effect of phenol/H₂O₂ molar ratios (2:1, 1:1, 1:2 and 1:3) on the conversion of phenol, the selectivities to CAT, HQ and BQ for the phenol hydroxylation catalyzed by Cu-ALG-3 was studied. As shown in Table 4, under the given experiment conditions, the conversion of phenol increased from 16.1% to 57.3% as the phenol/H₂O₂ molar ratio was changed from 2:1 to 1:3, which could be due to the increase in hydroxyl radical concentration upon decomposition of H₂O₂. However, when the phenol/H₂O₂ molar ratio was lower than 1:2, the selectivity to dihydroxybenzene decreased apparently, and the lowest selectivity to dihydroxybenzene (94.1%) was obtained at the phenol/H₂O₂ molar ratio being 1:3. The above result suggested that a large amount of oxidant was not an essential condition in improving the catalytic performance of the catalyst. In order to obtain a higher selectivity to dihydroxybenzene under the given catalytic system, the molar ratio of phenol/H₂O₂ should be controlled at 1:2.

3.2.2.5. The influence of the amount of catalyst. The influence of the catalyst amount on the hydroxylation of phenol was also studied. Three amounts of catalyst viz. 10, 50 and 100 mg were used. These results showed that the phenol conversion increased from 19.6 to 62.4% when the catalyst amount increased continuously from 10 to 100 mg, but the selectivity to dihydroxybenzene decreased when the catalyst increased to 100 mg. The increased active catalytic sites may be considered to be responsible for these phenomena, which led to the fast decomposition of H₂O₂ and oxidize phenol to other products. Therefore, 50 mg of the catalyst was the optimum amount for hydroxylation of phenol in this case.

3.2.2.6. The influence of the initial pH. The effect of the initial pH has also been investigated in the reaction. From the result displayed in Fig. 6, both acidic and alkaline solutions have negative effect on the conversion of phenol. The conversion increased from 12.1% to 37.7% as the initial pH increased from 2 to 7, while went on increasing the pH to 12, the conversion decreased to 8.3%. An interesting discovery is that acidic solution could enhance the further oxidation of HQ to BQ, which lead to the selectivity of HQ decreasing, while alkaline solutions could increase the selectivity of HQ. The specific influence of initial pH on the hydroxylation reaction is expected to be further study.

3.2.2.7. Catalyst stability and reusability. The Cu-ALG-3, which has favorable catalytic activity, was used three times for phenol hydroxylation to investigate its reusability (Fig. 6). The hydroxylation reaction was repeated three times under the condition: the amount ratio of phenol to catalyst was 20:1 and the molar ratio of phenol to H₂O₂ was 1:2. After each run, the spent catalyst was recovered by filtration, washed thoroughly with ethanol and dried. The weighed masses of the Cu-ALG-3 catalyst were 50, 44 and 37 mg, corresponded to the conversions of phenol were 52.7%, 47.7% and 44.4%, for the 1st, 2nd and 3rd runs, respectively. The selectivities of CAT to HQ were all 3:2. Combining the results of the

Table 4
Effect of molar ratio of phenol/H₂O₂ in the phenol hydroxylation.

Entry	Molar ratio of phenol/H ₂ O ₂	$X_{\text{phenol}} (\%)^{\text{a}}$	Selectivity (%) ^b		
			CAT	HQ	BQ
1	2:1	16.1	55.1	44.4	0.5
2	1:1	35.2	55.9	43.2	0.9
3	1:2	52.7	59.5	38.4	2.1
4	1:3	57.3	54.9	39.2	5.9

^a Phenol, 1.0 g; catalyst, 50 mg; water, 30 mL; 60 °C; 2 h.

^b Product distribution given on a tar-free basis.

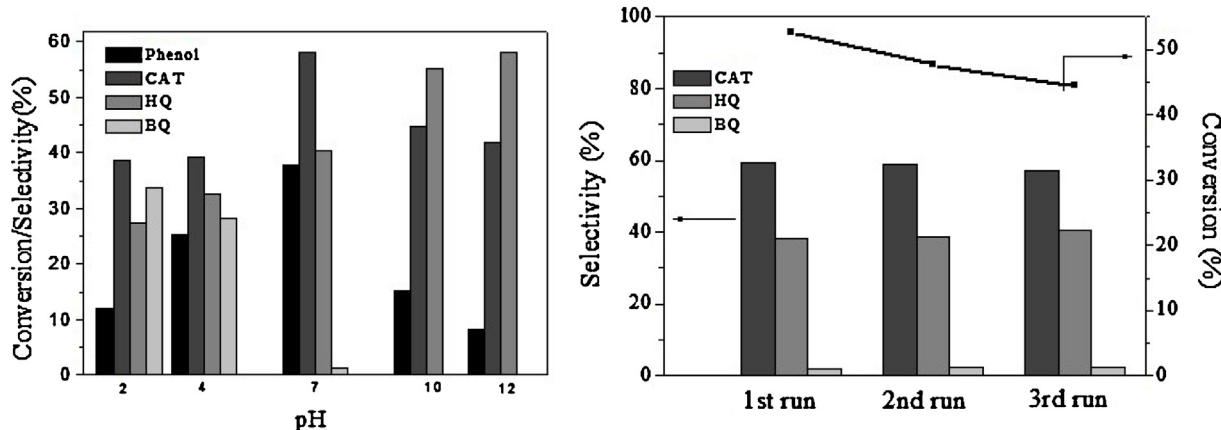


Fig. 6. Effect of pH on the phenol hydroxylation (left) and the catalytic performance of Cu-ALG-3 in the phenol hydroxylation reaction for three runs (right).

ICP-AES (Table 1) and mapping of Cu element of the catalyst (Fig. 4), the leaching amount of metal ions was little, but the mapping indicated that the detected Cu on the surface reduced significantly after reaction. Therefore, the reduction of the activity of the Cu-ALG catalyst should be attributed to both the loss of the catalyst during the recycling processes and the surface's coverage by tarry byproducts.

4. Conclusion

A series of metal crosslinked alginates catalysts have been synthesized and characterized, of which the result illustrated that the metal ions had crosslinked in the alginate structure successfully. Their catalytic activities for hydroxylation of phenol with H₂O₂ as an oxidant in water have been studied. The results illustrated that the catalytic activity of Cu-ALG catalyst was the highest and the leaching amount of metal between reactions was small. The catalytic performance of Cu-ALG catalyst was associated with the immobilized content of the Cu²⁺ ions. Furthermore, different reaction conditions of phenol hydroxylation catalyzed by the Cu-ALG-3 catalyst have been studied, the results illustrated that the catalyst exhibited wonderful catalytic performance for phenol hydroxylation under the following conditions: catalyst 50 mg, phenol/H₂O₂ molar ratio 1:2, solvent water, temperature 60 °C, time 2 h, initial pH 7. The results of the reusability experiment of Cu-ALG-3 indicated that the catalyst retained the majority of its initial activity after simple treatment. This study would be valuable for developing a new environmentally benign catalyst for oxidation of phenol.

Acknowledgments

This work was supported by the Natural Science Fund Council of China (21203013). The authors gratefully acknowledge the Centre of Analysis and Testing of Northeast Normal University for providing the ICP-AES analysis and Changchun University of Technology for all of the support that was provided.

References

- [1] L.J. Jian, C. Chen, F. Lan, S.J. Deng, W.M. Xiao, N. Zhang, Solid State Sci. 13 (2011) 1127–1131.
- [2] J.N. Muggo, S.F. Mapolie, J.L. van Wyk, Inorg. Chim. Acta 363 (2010) 2643–2651.
- [3] G. Wu, X.Y. Tan, G.Y. Li, C.W. Hu, J. Alloys Comp. 504 (2010) 371–376.
- [4] S. Ray, S.F. Mapolie, J. Darkwa, J. Mol. Catal. A: Chem. 267 (2007) 143–148.
- [5] H.S. Abbi, S.J.J. Titinchi, Appl. Catal. A 435–436 (2012) 148–155.
- [6] O.J. Kerton, P. Morn, D. Bethell, F. King, F. Hancock, A. Burrows, C.J. Kiely, S. Ellwood, G. Hutchings, Phys. Chem. Chem. Phys. 7 (2005) 2671–2678.
- [7] S. Li, G.L. Li, G.Y. Li, G. Wu, C.W. Hu, Microporous Mesoporous Mater. 143 (2011) 22–29.
- [8] K.M. Parida, S. Mol Mallick, J. Mol. Catal. A: Chem. 279 (2008) 104–111.
- [9] L.F. Gou, C.J. Murphy, Chem. Commun. 6 (2005) 5907–5909.
- [10] V. Rives, A. Dubey, S. Kannan, Phys. Chem. Chem. Phys. 3 (2001) 4826–4836.
- [11] C.X. Chen, C.H. Xu, L.R. Feng, F.L. Qiu, J.S. Suo, J. Mol. Catal. A: Chem. 252 (2006) 171–175.
- [12] S. Kannan, A. Dubey, H. Knozinger, J. Catal. 231 (2005) 381–392.
- [13] E.A. Karakhanov, A.L. Maximov, Y.S. Kardasheva, V.A. Skorkin, S.V. Kardashev, V.V. Predeina, M. Yu Talanova, E.L. Luke, J.A. Seeley, S.L. Cron, Appl. Catal. A 385 (2010) 62–72.
- [14] H.L. Tang, Y. Ren, B. Yue, S.R. Yan, H.Y. He, J. Mol. Catal. A: Chem. 260 (2006) 121–127.
- [15] S.A. Song, W. Zhao, L.N. Wang, J.L. Chu, J.K. Qu, S.H. Li, L. Wang, T. Qi, J. Colloid Interface Sci. 354 (2011) 686–690.
- [16] G.Y. Zhang, J.L. Long, X.X. Wang, Z.Z. Zhang, W.X. Dai, P. Liu, Z.H. Li, L. Wu, X.Z. Fu, Langmuir 26 (2010) 1362–1371.
- [17] X.Y. Qi, L.L. Zhang, W.H. Xie, T.H. Ji, R.G. Li, Appl. Catal. A 276 (2004) 89–94.
- [18] H.S. Abbo, S.J.J. Titinchi, Top Catal. 53 (2010) 254–264.
- [19] M.R. Maurya, S.J.J. Titinchi, S. Chandra, J. Mol. Catal. A: Chem. 214 (2004) 257–264.
- [20] J.S. Yang, Y.J. Xie, H. Wen, Carbohydr. Polym. 84 (2011) 33–39.
- [21] M. Robitzer, L. David, C. Rochas, F. Di Renzo, F. Quignard, Langmuir 24 (2008) 12547–12552.
- [22] M.S. Ikuko, M. Yasushi, N. Hideo, Biomed. Mater. 4 (2009) 1–8.
- [23] K.I. Draget, C. Taylor, Food Hydrocolloids 25 (2011) 251–256.
- [24] B.T. Stokke, O. Smidsrød, P. Bruheim, G. Skjak-Bræk, Macromolecules 24 (1991) 4637–4645.
- [25] E. Torres, Y.N. Mata, M.L. Blázquez, J.A. Muñoz, F. González, A. Ballester, Langmuir 21 (2005) 7951–7958.
- [26] M. Grace, N. Chand, S.K. Bajpai, J. Eng. Fiber. Fabr. 4 (2009) 24–35.
- [27] K.R. Reddy, K. Rajgopal, M.L. Kantam, Catal. Lett. 114 (2007) 36–40.
- [28] K.R. Reddy, N.S. Kumar, P.S. Reddy, B. Sreedhar, M.L. Kantam, J. Mol. Catal. A: Chem. 252 (2006) 12–16.
- [29] Y.C. Dong, W.J. Dong, Y.N. Cao, Z.B. Han, Z.H. Ding, Catal. Today 175 (2011) 346–355.
- [30] S.K. Papageorgiou, E.P. Kouvelos, E.P. Favvas, A.A. Sapalidis, G.E. Romanos, F.K. Katsaros, Carbohydr. Res. 345 (2010) 469–473.
- [31] Y.J. Jiang, Q.M. Gao, Mater. Lett. 61 (2007) 2212–2216.
- [32] K.M. Shaju, G.V. Subba Rao, B.V.R. Chowdari, Electrochim. Acta 48 (2002) 145–151.
- [33] P.X. Sheng, Y.P. Ting, J.P. Chen, L. Hong, J. Colloid Interface Sci. 275 (2004) 131–141.
- [34] A.P. Grosvenor, B.A. Kobe, M.C. Biesinger, N.S. McIntyre, Surf. Interface Anal. 36 (2004) 1564–1574.
- [35] A.M. Venezia, V. La Parola, G. Deganello, B. Pawelec, J.L.G. Fierro, J. Catal. 215 (2003) 317–325.
- [36] M.T. Cook, G. Tzortzis, D. Charalampopoulos, V.V. Khutoryanskiy, Biomacromolecules 12 (2011) 2834–2840.
- [37] J. Fernandez, M.R. Dhananjeyan, J. Kiwi, Y. Senuma, J. Hilborn, J. Phys. Chem. B 104 (2000) 5298–5301.
- [38] R. Lagoa, J.R. Rodrigues, Biochem. Eng. J. 46 (2009) 320–326.
- [39] F.W. Shi, Y.G. Chen, L.P. Sun, L. Zhang, J.L. Hu, Catal. Commun. 25 (2012) 102–105.
- [40] J.L. Hu, K.X. Li, W. Li, F.Y. Ma, Y.H. Guo, Appl. Catal. A 364 (2009) 211–220.
- [41] L.L. Lou, S.X. Liu, Catal. Commun. 6 (2005) 762–765.
- [42] M.G. Clerici, G. Bellussi, U. Romano, J. Catal. 129 (1991) 159–167.
- [43] A. Dubey, V. Rives, S. Kannan, J. Mol. Catal. A: Chem. 181 (2002) 151–160.